the plant journal

SEB Society for Experimental Biology

The Plant Journal (2015) **81,** 453–466 doi: 10.1111/tpj.12742

DASH transcription factor impacts *Medicago truncatula* seed size by its action on embryo morphogenesis and auxin homeostasis

Mélanie Noguero[1,†], Christine Le Signor[1,†], Vanessa Vernoud[1], Kaustav Bandyopadhyay[2], Myriam Sanchez[1], Chunxiang Fu[2,‡], Ivone Torres-Jerez[2], Jiangqi Wen[2], Kirankumar S. Mysore[2], Karine Gallardo[1], Michael Udvardi[2], Richard Thompson[1] and Jerome Verdier[2,3,*]

[1]*INRA, UMR1347 Agroécologie, pôle GEAPSI, BP 86510, F-21000 Dijon, France,*

[2]*Plant Biology Division, The Samuel Roberts Noble Foundation, 2510 Sam Noble Parkway, Ardmore, OK 73401, USA, and*

[3]*Shanghai Center for Plant Stress Biology, Shanghai Institutes of Biological Sciences, Chinese Academy of Sciences, 3888 Chenhua road, 201602 Shanghai, China*

Received 13 September 2014; revised 30 November 2014; accepted 2 December 2014; published online 10 December 2014.

*For correspondence (e-mail javerdier@icloud.com).

†These authors contributed equally to this work.

‡Present address: Qingdao Institute of Bioenergy and Bioprocess Technology, Chinese Academy of Sciences (QIBEBT, CAS), No. 189 Songling Road, Laoshan District, Qingdao 266101, China.

SUMMARY

The endosperm plays a pivotal role in the integration between component tissues of molecular signals controlling seed development. It has been shown to participate in the regulation of embryo morphogenesis and ultimately seed size determination. However, the molecular mechanisms that modulate seed size are still poorly understood especially in legumes. *DASH* (*DOF Acting in Seed embryogenesis and Hormone accumulation*) is a DOF transcription factor (TF) expressed during embryogenesis in the chalazal endosperm of the *Medicago truncatula* seed. Phenotypic characterization of three independent *dash* mutant alleles revealed a role for this TF in the prevention of early seed abortion and the determination of final seed size. Strong loss-of-function alleles cause severe defects in endosperm development and lead to embryo growth arrest at the globular stage. Transcriptomic analysis of *dash* pods versus wild-type (WT) pods revealed major transcriptional changes and highlighted genes that are involved in auxin transport and perception as mainly under-expressed in *dash* mutant pods. Interestingly, the exogenous application of auxin alleviated the seed-lethal phenotype, whereas hormonal dosage revealed a much higher auxin content in *dash* pods compared with WT. Together these results suggested that auxin transport/signaling may be affected in the *dash* mutant and that aberrant auxin distribution may contribute to the defect in embryogenesis resulting in the final seed size phenotype.

Keywords: endosperm, seed size, embryogenesis, *Medicago truncatula*, auxin.

INTRODUCTION

During seed development, the tissues that surround the developing embryo play important roles in determining both final seed size and composition, as shown by mutant phenotypes in *Arabidopsis thaliana*, *Medicago truncatula* and *Pisum sativum* (Luo *et al.*, 2005; Adamski *et al.*, 2009; D'Erfurth *et al.*, 2012). In most angiosperms, endosperm development is divided into two phases: (1) a syncytial phase with nuclear divisions without cytokinesis immediately after fertilization; and (2) a cellularization phase, which gives rise to three distinct domains: (i) the micropylar region close to the embryo; (ii) the central region forming the largest part of endosperm; and (iii) the chalazal region involved in the transfer of maternal nutrients to embryo and/or endosperm. In contrast with cereals, the endosperm of most dicotyledonous seeds, including legumes, is a transient structure, undergoing cell breakdown during seed filling to leave only a single layer of endosperm cells at maturity. However, whilst being a non-storage tissue at maturity, the endosperm has an important role to play in nourishing the developing embryo (Ingram, 2010; Hehenberger *et al.*, 2012) and thus indirectly affects final seed content and seed size.

Final seed size has been shown to depend on a complex crosstalk between the endosperm and the integuments during early post-fertilization seed expansion (Garcia *et al.*, 2005). Several genes have been shown to be essential for proper development of both endosperm and embryo. For instance, *HAIKU2 (IKU)* is a leucine-rich repeat receptor-like kinase (LRR-RLK) expressed specifically in endosperm and *iku* mutants displayed precocious endosperm cellularization and decrease in embryo cell size, resulting in smaller seeds (Luo *et al.*, 2005). Similar phenotypes regarding endosperm cellularization and embryo cell division have been observed in several mutants such as *keule* (Assaad *et al.*, 1996), *knolle* (Lauber *et al.*, 1997), and *hinkel* (Strompen *et al.*, 2002) implying a link between endosperm cellularization and embryo cytokinesis. A recent study showed that the Arabidopsis peptide ligand CLAVATA3/EMBRYO SURROUNDING REGION 8 (CLE8), which is restricted in its expression to the young embryo and endosperm, regulates both embryo cell divisions and endosperm proliferation (Fiume and Fletcher, 2012). Thus, in addition to its conduction of nutrients, the endosperm appears to coordinate via signal transmission the development of the three seed compartments.

Regarding the role and mode of action of plant hormones during early seed/pod development and specifically in the endosperm, reports are scanty. Auxin is important for several major steps of embryo specification in both the apical and basal domains (Möller and Weijers, 2009). The auxin involved appears to be synthesized in the embryo and distributed throughout the embryo in gradients established by the PIN family of efflux carriers (Cheng *et al.*, 2007; Robert *et al.*, 2013). Cytokinin and auxin has been showed to play a role in endosperm differentiation. High cytokinin concentration due to overproduction of isopentenyltransferase (IPT) caused a mosaic aleurone phenotype (Geisler-Lee and Gallie, 2005). Accumulation of auxin due to auxin transport inhibition by *N*-1-naphthylphthalamic acid (NPA) caused multiple aleurone layers to develop (Forestan and Varotto, 2011). More recently, the *CKX2* gene, encoding a cytokinin oxidase 2 involved in cytokinin degradation, has been shown to be a direct target of the IKU pathway controlling early endosperm growth (Li *et al.*, 2013). Moreover, an auxin (IAA)-deficient maize mutant, de-B18, has 30% less seed mass than the WT due to a defect in early endosperm differentiation (Forestan *et al.*, 2010).

In a previous study we identified several seed-specific TF that were expressed in the endosperm tissue of *Medicago truncatula* (Verdier *et al.*, 2008). Among them was a DNA-binding with One Finger (DOF) protein, which belongs to the zinc finger TF family, widely distributed within the *Viridiplantae* but absent from other eukaryotes (Moreno-Risueno *et al.*, 2007). The DOF TFs are characterized by a highly conserved DOF domain of 52 amino acids, essential for DNA binding (Yanagisawa, 2002) and in some cases for protein–protein interactions, although the C-terminal is also involved in this interaction (Diaz *et al.*, 2002). The DOF family is implicated in a wide range of processes essential for seed germination, seed maturation and plant development, including plant defences against pathogens (reviewed in Noguero *et al.*, 2013) .

In this study, we have functionally characterized a *M. truncatula* endosperm-specific DOF TF, called hereafter *DASH* (*DOF Acting in Seed embryogenesis and Hormone accumulation*) expressed in the developing seed at the transition phase between embryogenesis and seed filling (Verdier *et al.*, 2008). We have exploited two series of mutants, a TILLING resource created in the *M. truncatula* reference line A17 (Le Signor *et al.*, 2009), and a *Tnt1* transposon insertion library, constructed in the R108 line preferred for genetic transformation of *M. truncatula* (Cheng *et al.*, 2014). Cytological analyses demonstrated that *dash* mutation severely affects embryo morphogenesis, and the transcriptomes of loss-of-function mutants highlighted severe changes in molecular processes related to early stages of seed/pod development. Most notably, *dash* pods accumulated high concentrations of auxin despite their retarded development, suggesting a defect in auxin homeostasis.

RESULTS

DASH encodes an endosperm-specific DOF transcription factor

In a previous study (Verdier *et al.*, 2008), a DOF TF gene (Medtr2g014060, *DASH*) was identified due to its seed expression restricted to the endosperm. *DASH* relative expression was evaluated in A17 and R108 *M. truncatula* seeds between 4 and 14 days after pollination (DAP) by quantitative reverse transcription polymerase chain reaction (qRT-PCR) (Figure 1a). *DASH* mRNA was first detected at 6 DAP, corresponding to the embryogenesis phase, in which the embryo is at the globular stage and cell-type differentiation begins. mRNA levels increased by 8 DAP (late globular-heart stage) to reach a maximum abundance at 12 DAP (linear cotyledon stage), when after extensive cell divisions (i.e. embryogenesis), seed storage proteins start to accumulate along with embryo cell expansion (i.e. seed filling) (Gallardo *et al.*, 2007). This expression profile suggested a role for this TF during the terminal phase of embryogenesis. Using the comprehensive dataset available at the *M. truncatula* Gene Expression Atlas web server (MtGEA, http://mtgea.noble.org) (Benedito *et al.*, 2008), we confirmed that *DASH* expression (probe set Mtr.21255.1.S1_at) was absent in other plant tissues and that this TF was not expressed during the latest stages of seed development (Figure S1a). qRT-PCR experiments on dissected seed and pod tissues at 12 DAP confirmed that

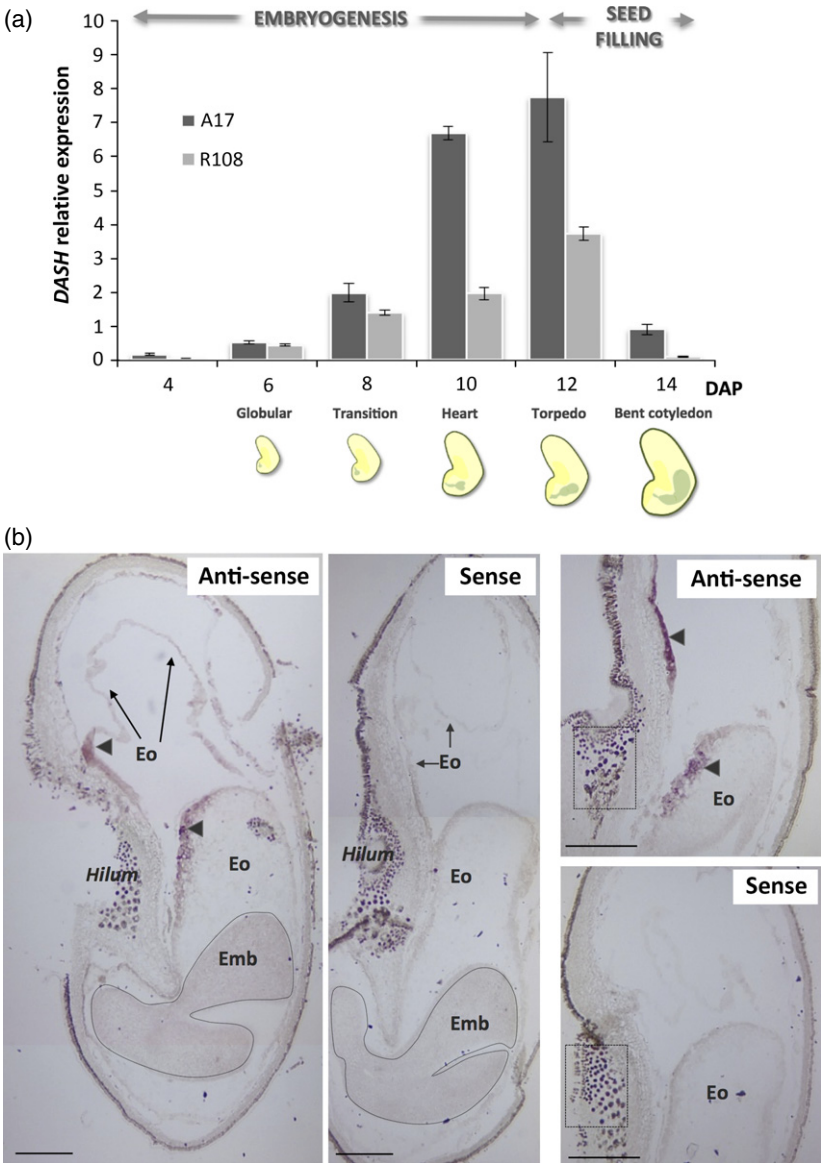

Figure 1. *DASH* expression during seed development.
(a) *DASH* relative expression levels in *Medicago truncatula* A17 and R108 through early seed development (in Days After Pollination, DAP). *DASH* relative transcript abundance was measured by qRT-PCR. Expression levels were obtained by normalization with the *MSC27* and *PDF2* genes (Verdier *et al.*, 2008). Data are average values ± standard deviation (SD) from three biological replicates carried out in technical replicates.
(b) *In situ* hybridization of 12 DAP seed using a *DASH*-specific anti-sense probe. The signal (purple colour) is located in the chalazal region of the endosperm (arrowheads). Negative control with the sense probe did not yield to any signal in the endosperm. Dotted squares show background in hilum region, found with both sense and anti-sense probes. Endosperm and embryo are indicated respectively by Eo and Emb and by arrows. Scale bars = 250 μm.

DASH was preferentially expressed in seeds compared with pod wall (Figure S1b).

Further exploration of *DASH* expression was carried out by *in situ* hybridization on 12 DAP A17 seeds. The endosperm appeared split in two parts: one attached to the seed coat and another surrounding the embryo, as previously observed for early developing *M. truncatula* seeds (D'Erfurth *et al.*, 2012), the endosperm being delicate and hence difficult to keep intact during steps of tissue preparation for *in situ* hybridization. *DASH* expression was restricted to a specific zone of the endosperm corresponding to the chalazal region, close to the hilum, which corresponds to the point of attachment of the seed to the pod (Figure 1b).

A distance analysis between DOF proteins from *M. truncatula* (Noguero *et al.*, 2013) and other species was carried out using the neighbor-joining method. The corresponding tree divided into eight clusters (A–H; Figure S2), which partially match with the classification of Arabidopsis DOF proteins (Yanagisawa, 2002). DASH protein, which belongs to group E, clustered with several soybean and pea DOF TFs. Interestingly none of the members of this group currently has a function ascribed to them.

dash loss-of-function alleles have a seed-lethal or near-lethal phenotype

Two *M. truncatula* mutant populations were screened to identify mutations in *DASH.* From the EMS population (le Signor *et al.*, 2009), line EMS109 (G177A) was characterized by the apparition of a stop codon (W59STOP) just after the loop within the DOF domain (Figure S3). This mutation causes a dramatic change in protein sequence by

truncation of the DOF domain, resulting in a predicted peptide length of only 59 amino acids instead of 336 for the full-length protein sequence. In addition, two insertion mutant lines were identified from the *Tnt-1* insertion mutant population generated in the R108 genotype (Tadege *et al.*, 2008). These insertions were located in the putative promoter region, at −342 bp (mutant NF5285) and at −151 bp (NF6042) upstream of the ATG start codon (Figure S3).

Phenotypes of the different mutants compared with their respective WT lines were studied. While NF6042 and EMS109 exhibited seed-lethal phenotypes, NF5285 displayed a mild seed phenotype in the homozygous state with a reduction of 16% of the mature seed weight (Table 1).

Heterozygous plants with the NF6042 insertion located at −151 bp were analysed by PCR-based genotyping and no homozygous plant could be recovered from the progeny. The observed 2:1 segregation ratio between heterozygous and WT plants among the progeny of self-fertilized heterozygous plants suggested that NF6042 insertion was embryo-lethal at the homozygous state (Figure S4a). To investigate this further, young developing pods of self-fertilized NF6042 heterozygous plants were dissected and small and/or dry seeds were observed within pods in a proportion close to 3:1 (Figure S4b), consistent with Mendelian segregation of a single recessive allele and confirming homozygous seed-lethality. The observed reduction of seed number in mature pods from self-pollinated heterozygotes is also consistent with the segregation of a seed-lethal allele. The same genetic analysis was performed for the EMS109 segregating population and led to similar results (Figure S4a,b). However, one homozygous plant was obtained out of 100 progenies from self-fertilized heterozygous EMS109 plants. Compared with the WT, we observed that the EMS109 mutation in the homozygous state caused pod abortion during the first months of the plant life cycle: flowers appeared normally, but after 10–12 days small developing pods aborted, dried out and detached (Figure 2a). These pods were much smaller than the WT pods at the same stage and contained smaller seeds (Figure 2b,c). Interestingly, at the end of the plant life cycle (after 2 or 3 months of flowering), EMS109 homozygous plants were able to produce mature pods, which were smaller than WT but contained viable seeds. The weight of these seeds was greatly reduced compared with WT (67%; Table 1 and Figure 2d) and the number of seeds per pod was also reduced compared with WT plants (Table 1). These small seeds gave rise to abnormal cup-shaped cotyledon phenotypes in about 40% of cases (Figure 2e), and most of these abnormal seedlings did not give a viable plant.

DASH expression analysis in different mutant lines using qRT-PCR revealed a dramatic decrease of *DASH* expression in EMS109 mutant seeds (i.e. null mutant, Figure S4d) and a slight decrease in NF5285 mutant seeds at 10 DAP (i.e. knock-down mutant, Figure S4e). No homozygous plant was isolated for the NF6042 line but a decrease of 40% of *DASH* expression in seeds dissected from heterozygous NF6042 pods was measured by qRT-PCR compared with WT plants at the same stage (Figure S4f)

In order to definitively link the seed phenotype to the *dash* mutation, complementation of the *dash* mutant was carried out using the EMS109 mutant line. A construct containing the native promoter sequence fused to the open reading frame of *DASH* was introduced into the homozygous EMS109 mutant line using *Agrobacterium tumefaciens*. Among second generation transformant lines containing the *pDASH::DASH* construct selected in the presence of the selection marker, two lines (i.e. EMS109 Compl A and EMS109 Compl B) displayed complementation of the seed-lethal phenotype and a restoration of the normal seed weight (Figure S5). These complemented lines did not show any defective reproductive phenotypes in the next generations such as those observed in EMS109 mutants.

dash mutants are impaired in embryogenesis

The seed-lethal phenotype prompted us to study in more detail embryo development of the *dash* mutants. Seeds were dissected from developing pods, cleared and

Table 1 Phenotype description of the EMS and *Tnt1 dash* mutants

Mutant	Genotype	Seed weight (mg)	Seed weight reduction/ WT (%)	Pod weight (mg)	Number of seeds per pod
EMS109	*dash/dash* [a]	1.43 ± 0.042*	67	35.5 ± 1.54*	6 ± 0.23*
	dash/DASH	3.99 ± 0.057*	9	61.1 ± 1.84*	6 ± 0.28*
	DASH/DASH	4.37 ± 0.072	16	73.8 ± 2.07	8 ± 0.24
NF5285	*dash/dash*	3.87 ± 0.187*	10	127.2 ± 5.12*	6 ± 0.3*
	DASH/DASH	4.61 ± 0.103		169 ± 8.25	7 ± 0.3
NF6042	*dash/DASH* [b]	3.53 ± 0.07*		71.58 ± 5.1	5 ± 0.45*
	DASH/DASH	3.94 ± 0.05		76.8 ± 3.9	8 ± 0.24

[a]Seed production in the late stage of the plant life cycle.
[b]Homozygous has a seed-lethal phenotype.
*Significant value relative to wild-type ($P < 0.05$, Student's *t*-test).

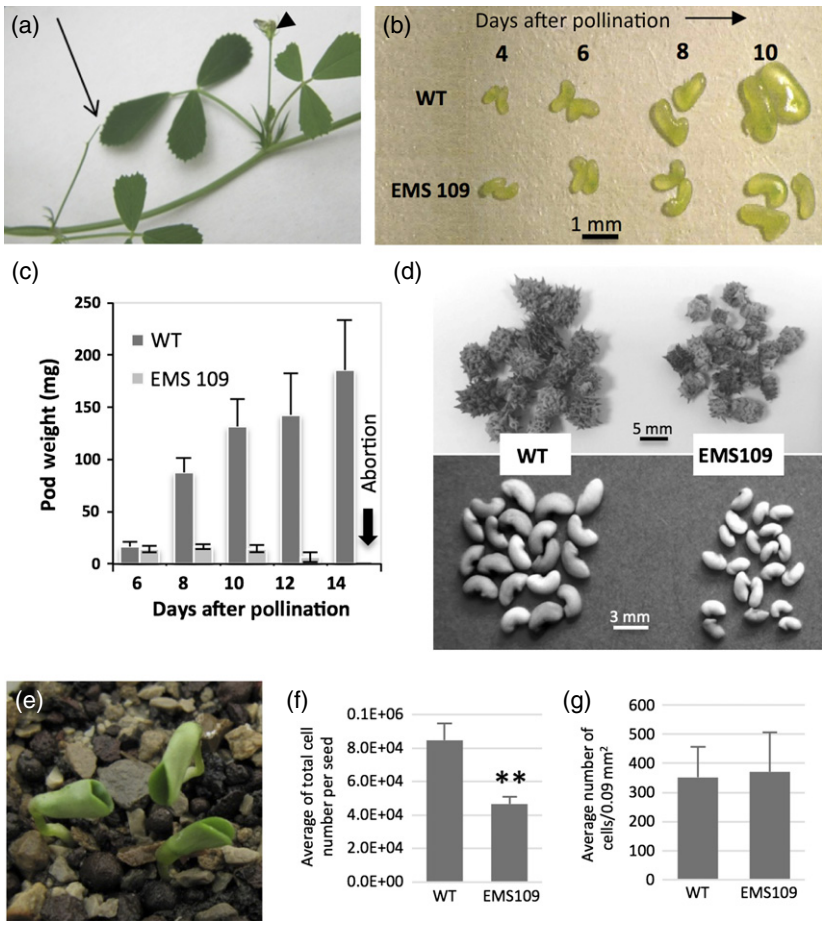

Figure 2. Phenotype of the homozygous EMS109 mutant.
(a) Pod abortion during the first months of the plant life cycle.
(b) Seed development from 4 DAP to 10 DAP for wild-type (top) and EMS109 mutant (bottom).
(c) Kinetics of pod weight from 6 DAP to 12 DAP for wild-type and EMS109.
(d) Comparison of mature pod and seed sizes from WT (left) and EMS 109 mutant (right) at the end of the plant life cycle.
(e) Abnormal mutant seedlings showing cup-shaped cotyledons.
(f) Cell number per seed from WT and EMS 109 mutant at the mature stage.
(g) Cell size calculated by the number of cells per 0.9 square mm from WT and EMS 109 mutant at the mature stage.

observed using differential interference contrast (DIC) microscopy. A developmental series of WT A17 (A–D) and EMS109 mutant (E–L) cleared seeds is presented in Figure 3. Figure 3(e–h) shows mutant seeds before abortion harvested from 5-week-old plants (i.e. beginning of the plant cycle) while Figure 3(i–l) show seeds harvested on plants at the end of their life cycle that were ultimately able to produce small mature seeds. For seeds harvested from 5-week-old plants, no change was observed in embryo development until 6 DAP (Figure 3a,e); whereas at 8 DAP, we observed a delay in embryo development (Figure 3b,f), coinciding with the beginning of *DASH* gene expression. At 10 DAP, WT embryos reached heart stage whereas EMS109 embryos were still at the globular stage, attesting embryo growth arrest (Figure 3c,g). Cellularized endosperm appeared between 6 and 10 DAP in WT but gradually degenerated in EMS109 mutants (Figure S6) leading to small seeds, tissue collapse and desiccation (Figure 3h). The smallest seeds from developing heterozygous NF6042 pods (Q–T) were also cleared and compared with WT R108 seeds (M–P) in Figure 3 and similar results as those seen for EMS109 were observed, with a delay in embryo development from 8 DAP resulting in embryo growth arrest at the globular stage. Regarding the weak allele NF5285, we observed a slight delay in embryo development from 10 DAP onward (Figure S7).

The EMS109 mutant seeds collected at the end of the plant life cycle, that escaped abortion, differed from WT seeds by their smaller size, as previously shown in Figure 2d, and their fused cotyledons (Figures 2e and 3k,l). By counting the number of embryo cells per square mm in the EMS109 mutant mature seeds that escaped abortion, we did not observe any variation in cell size compared with the WT. However, the total number of cells per seed determined using a haemocytometer after enzymatic digestion was significantly reduced. These results suggest that the number of cell divisions decreased in the mutant embryos, whereas cell elongation was not affected (Figure 2f,g).

A transcriptome comparison of WT and EMS109 mutant pods reveals major transcriptional changes in the *dash* mutant

To get an insight into the processes affected in developing *dash* seeds, we used the *M. truncatula* Affymetrix GeneChips for hybridization of RNA extracted from the WT and EMS109 mutant pods at 8 DAP (about 3–4 days before pod abortion). At this stage, both *dash* and WT embryos are in globular stages with *dash* embryos being slightly smaller.

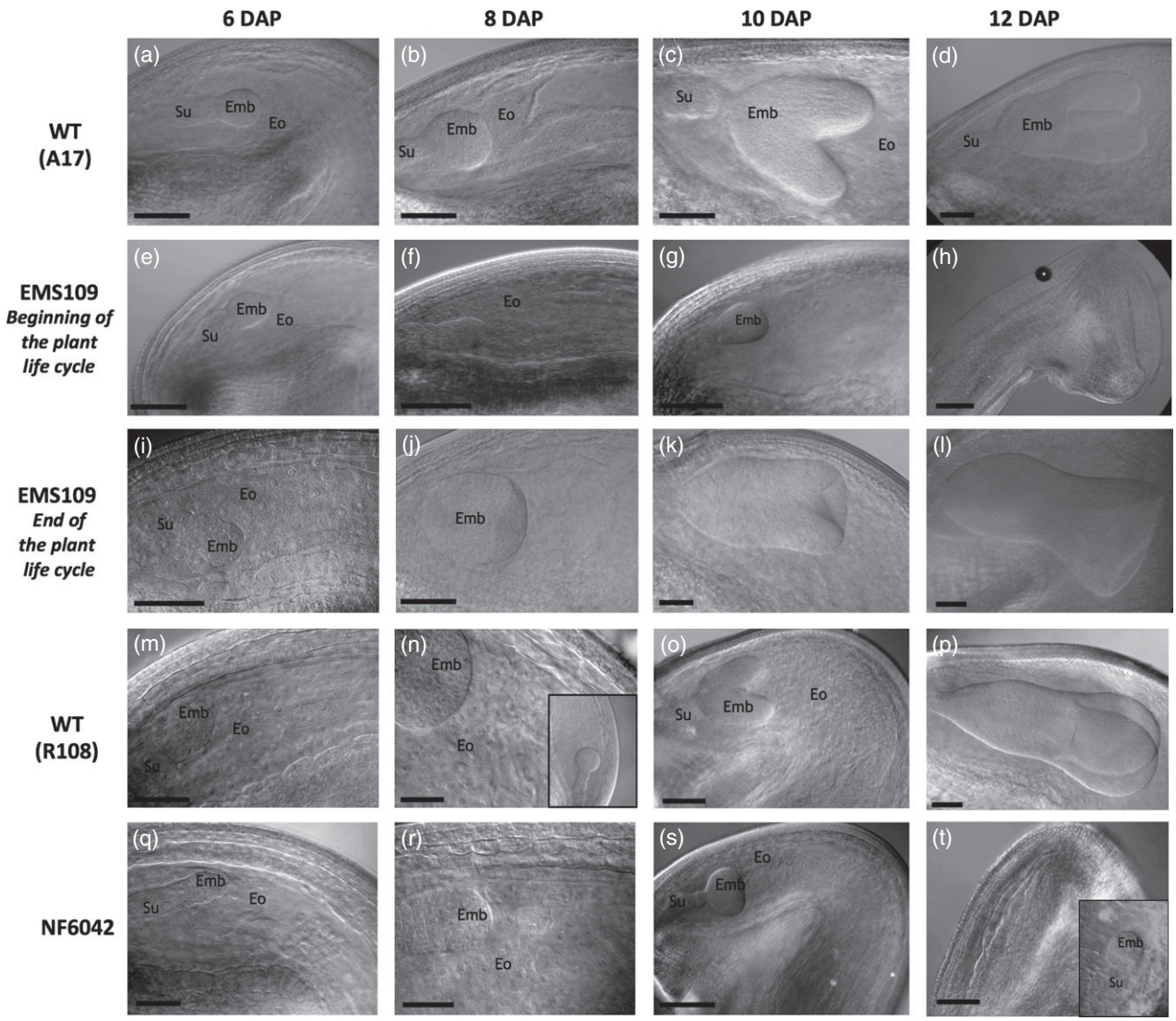

Figure 3. Embryo growth arrest in EMS109 and NF6042 mutants.
Cleared pictures of embryo and endosperm during early seed development. Wild-type A17 seeds (a–d), EMS109 seeds at the beginning of plant life cycle (e–h) and EMS109 seeds escaped from abortion at the end of the plant life cycle (i–l).Wild-type R108 seeds (m–p) and small seeds dissected from heterozygous NF6042 pods (q–t). Emb, embryo; Eo, endosperm; Su, suspensor. Scale bar = 100 μm except for pictures (i, m, n, q, r) (50 μm).

Following log transformation of the data and *t*-test correction, a probe set list of 7452 genes differentially expressed between the *dash* mutant and the WT were selected: 3766 were down-regulated and 3686 up-regulated. The exhaustive list of these genes is presented in Table S1. Schematic PAGEMAN representation of under- and over-represented BIN classes [i.e. functional classes (Thimm *et al.*, 2004)] revealed major effects on most metabolic pathways (Table 2).

Protein synthesis (mainly ribosomal proteins), auxin pathways and auxin response genes, cell cycle (cyclin-dependent protein kinase regulator) and chromatin structure (nucleosome assembly, DNA binding or DNA replication factor and histone synthesis) were the most down-regulated functional classes in *dash* (score ≤5, Table 2). Besides the down-regulation of specific metabolic pathway/classes, we searched for the most strongly down-regulated genes in *dash* (log2 expression ratio between *dash* and WT ≤3.5). A smaller number of genes (12) was identified, of which eight displayed an expression pattern similar to *DASH* (i.e. seed specific with an expression peaking between 10 and 12 DAP; Figure 4a). Two of them (Mtr.1254.1.S1_at, Mtr.21576.1.S1_at) corresponded to short cysteine-rich proteins (CRPs). Down-regulation of these two genes was confirmed in *dash* seed tissues at 8 DAP by qRT-PCR (Figure 4b) and expression of the most deregulated one (Mtr.21576.1.S1_at) was shown by *in situ* hybridization to be restricted to the chalazal endosperm, a pattern identical to that of *DASH* (Figures 1b and 4c). Although the other three genes (Mtr.19455.1.S1_at,

Table 2 PAGEMAN display of over-represented categories deregulated in 8 DAP *dash* pods compared with WT. Log_2 ratio of mutant data versus WT data from three replicates. Only classes with significant changes according to the normalized Wilcoxon test (= score) are represented. Data from the *Medicago* Gene Expression Atlas (Benedito *et al.*, 2008) were normalized and added

Functional class	Score	Leaf	Petiole	Veg bud	Stem	Flower	Pod (5–21)	Seed_ 10 dap	Seed_ 12 dap	Seed_ 16 dap	Seed_ 20 dap	Seed_ 24 dap	Seed_ 36 dap	Seed_ Coat (16–24 dap)	Root
Protein synthesis	−6.8	−51	−42	50	−12	−28	33	57	32	15	−1	−20	20	−60	8
Hormone metabolism auxin induced-regulated-responsive-activated	−6.0	35	33	−10	4	78	10	−17	−21	−24	−25	−23	−23	−11	−8
Hormone metabolism auxin	−5.8	26	29	−7	5	74	12	−15	−19	−21	−23	−22	−23	−9	−7
Cell	−5.4	−29	−16	21	5	−14	16	30	18	9	−4	−11	−17	−9	1
Cell cycle	−5.2	−46	−25	39	1	−21	28	55	32	12	0	−14	−28	−31	−1
DNA.synthesis/chromatin structure	−5.1	−37	−31	44	−18	−1	17	62	33	0	−18	−11	−2	−23	−14
Cell organisation	−3.4	−23	−11	12	11	−12	13	21	15	8	−5	−11	−20	0	4
Protein Folding	−3.4	−17	−17	56	−3	−24	29	38	17	−3	−19	−29	17	−41	−2
Nucleotide metabolism salvage	−3.1	−36	−22	60	26	−19	56	53	27	−1	−19	−35	−18	−45	−27
Protein degradation subtilases	−2.7	−15	12	11	29	11	24	33	3	−5	−15	−22	−35	−10	−20
misc GDSL-motif lipase	−2.6	2	13	47	12	28	12	−1	−15	−17	−19	−13	−13	−17	−19
Cell wall	−2.5	−11	22	8	30	21	21	2	−6	−6	−15	−20	−30	−11	−4
Lipid metabolism phospholipid synthesis	−2.3	74	11	30	−4	19	−1	14	−3	−17	−20	−31	−42	−5	−25
Signalling receptor kinases LRR III	−2.2	−20	−3	38	36	−4	40	18	8	−6	−19	−25	−42	−29	8
Protein targeting nucleus	−2.1	−52	−8	40	39	−41	41	59	35	−15	−31	−30	−9	−40	11
misc beta 1,3 glucan hydrolases	−2.1	−25	−18	21	11	−19	17	28	18	13	−4	−10	−36	14	−9
misc plastocyanin-like	−2.1	−33	−20	20	13	0	26	38	22	9	2	−4	−31	−27	−15
Signalling G-proteins	−2.1	−33	−17	22	10	−11	20	30	13	4	−6	−13	1	−29	10
RNA transcription	−2.0	−59	−40	32	−25	−21	−3	51	27	−5	−10	−7	94	−27	−7
Hormone metabolism cytokinin	2.0	−6	−18	−34	−13	59	−24	11	3	16	−10	−5	−2	53	−30
Development	2.2	−7	−2	−5	6	6	−3	−4	−4	−8	−8	−3	11	8	15
Lipid metabolism FA synthesis and FA elongation acyl coa ligase	2.2	−6	−5	28	3	−15	4	6	17	28	2	−17	−20	−16	−7
Hormone metabolism ethylene induced-regulated-responsive-activated	2.3	−21	−13	−30	−16	40	−19	0	−8	−8	−2	−4	7	33	41
Amino acid metabolism.synthesis.central AA metabolism	2.4	70	20	9	−9	−17	−23	−16	−10	−6	2	5	−24	5	−5
Hormone metabolism abscisic acid	2.6	27	6	−27	−18	4	−27	−8	−12	−3	−3	2	20	44	−5
misc cytochrome P450	2.7	19	6	−14	−12	32	−12	−10	−11	−13	0	1	7	−1	8
Amino acid metabolism degradation	2.7	−23	−14	−19	−20	19	−8	−18	−15	2	18	22	29	29	0
Hormone metabolism ethylene synthesis degradation	2.8	32	25	−12	−14	15	0	−9	−11	−8	−7	−6	3	7	−15
Protein degradation autophagy	2.9	−3	−11	−51	−39	37	−36	−28	−16	−19	2	17	31	71	45
Minor CHO metabolism	3.0	−27	−22	−24	−19	14	−4	_5	3	5	−4	−1	32	42	10
Protein posttranslational modification	3.1	−2	−4	−12	−6	8	−12	−3	−2	−3	−3	−1	−1	27	14
Transport	3.5	3	0	−9	3	24	5	−2	−3	−8	−10	−12	−6	2	13
Hormone metabolism ethylene	3.6	17	13	−8	−10	21	−1	−9	−11	−11	−7	−8	3	8	5
Not assigned	3.7	−6	−5	3	−1	0	4	5	0	−4	−5	−7	9	−1	8

Table 2

Functional class	Score	Leaf	Petiole	Veg bud	Stem	Flower	Pod (5–21)	Seed_ 10 dap	Seed_ 12 dap	Seed_ 16 dap	Seed_ 20 dap	Seed_ 24 dap	Seed_ 36 dap	Seed_ Coat (16–24 dap)	Root
Transport amino acids	3.9	17	16	−24	1	41	−5	−21	−25	−24	−21	−18	16	0	47
Protein degradation	6.5	35	−3	−13	−16	15	−7	3	0	−7	−5	−7	11	8	−13
Protein degradation ubiquitin	7.3	−15	−10	−31	−14	1	−26	−11	−11	−6	3	11	47	49	12

Mtr.2563.1.S1_at and Mtr.50101.1.S1_at) lacked clear annotations, sequences analysis revealed that they encode small peptides possessing signal peptides and several cysteine residues classifying them as CRPs. A further three other genes with expression patterns similar to *DASH* were down-regulated by 15- to 35-fold in *dash* pods compared with WT and encode non-specific lipid-transfer protein ns-LPT-like (Mtr.22353.1.S1_at), germin-like (Mtr.39975.1.S1_at) and desiccation-related protein (DRP; Mtr.42115.1.S1_at) (Figure 4a).

The most up-regulated functional classes in *dash* were protein degradation (mainly E3 ubiquitin ligases) and transport (mainly amino acid transporters orthologous to amino acid permeases, cationic amino acid transporters and proline transporters). Among the 10 most up-regulated genes, four of them corresponded to genes encoding NAC [NAM (no apical meristem), ATAF, CUC (cup-shaped cotyledon)]-domain TFs that were 40–90-fold up-regulated in *dash* (log2 ratio between 5.4 and 6.5, Figure 4a). These TFs are normally expressed in WT flowers and/or during seed filling (16–36 DAP) but are weakly expressed in early stages of seed development (Figure 4a), suggesting they could be indirectly repressed by *DASH.*

Auxin homeostasis and transport are impaired in *dash* mutants

Genes related to the functional class 'hormone', and particularly 'auxin', were among the most deregulated in the *dash* mutant (Table 2). Interestingly, most of the auxin-related genes were down-regulated in *dash* and notably 65% of them encode auxin-induced proteins (Table S2). Homologs of the auxin efflux carriers *AtPIN1 (MtPIN4)*, *AtPIN7 (MtPIN1 and MtPIN3) and AtPIN8 (MtPIN8)* were also down-regulated in *dash.* Consistent with these results, the Aux/IAA family was down-regulated in *dash.* Interestingly, among the few auxin-responsive genes up-regulated in *dash* was *IAA18-LIKE*, which alters *PIN1* expression in the Arabidopsis embryo (Ploense *et al.*, 2009) Finally, it is noteworthy that the genes related to auxin synthesis were not significantly deregulated in *dash* suggesting that auxin synthesis is not impaired in *dash* pods. In order to better understand the link between the *dash* mutation and the deregulation of auxin-responsive genes observed in the mutant transcriptome, auxin content was measured in EMS109 mutant and WT pods using liquid chromatography coupled with tandem mass spectrometry (LC-MS/MS). At 8 DAP, the stage used for transcriptomic analysis, IAA content was about 36 times higher in *dash* pods compared with WT (Figure 5a). Higher IAA content was still observed at 10 DAP in mutant pods, just before pod abortion occurring around 12 DAP. Interestingly, we also observed a higher accumulation of the auxin conjugate in 8 and 10 DAP mutant pods compared with WT, which corresponds to an inactive form of auxin potentially involved in IAA

(a)

	Probeset-Id	Mtv3.5	Annotation	Log2 8dap (dash/wt)	Root	Leaf	Petiole	VegBud	Stem	Flower	Pod	Seed_10 dap	Seed_12 dap	Seed_16 dap	Seed_20 dap	Seed_24 dap	Seed_36 dap	Seed_coat
Probes down	Mtr.2563.1.S1_at	BI271631	no protein match	−6.4	11	11	11	11	11	10	389	3627	2513	504	15	15	12	157
	Mtr.21576.1.S1_at	Medtr8g046040	Cysteine Rich Peptide (CRP)	−6.1	7	7	8	7	8	7	96	943	497	50	10	8	8	16
	Mtr.50101.1.S1_at	Medtr6g009690	no protein match	−5.7	21	23	23	24	24	28	116	1860	1106	148	25	28	31	51
	Mtr.19455.1.S1_at	Medtr6g009680	no protein match	−5.5	13	11	10	10	12	10	31	961	175	24	13	11	10	10
	Mtr.1254.1.S1_at	Medtr2g076980	Cysteine Rich Peptide (CRP)	−5.3	8	7	8	8	7	7	114	721	493	68	8	9	9	34
	Mtr.42115.1.S1_at	Medtr2g033520	Desiccation-related protein PCC13-62	−5.1	7	7	7	7	7	8	235	3073	1042	66	9	18	11	16
	Mtr.39975.1.S1_at	Medtr3g019680	Germin-like protein	−4.1	8	7	8	8	8	8	140	3121	1414	60	7	8	9	14
	Mtr.22353.1.S1_at	Medtr7g083580	Plant lipid transfer protein	−3.6	12	13	12	12	11	14	61	1828	1938	304	14	13	13	129
Probes up	Mtr.50038.1.S1_at	Medtr7g085220	ANAC018,ATNAM, NARS	5.4	29	72	19	12	11	1437	88	12	10	12	20	50	509	364
	Mtr.28491.1.S1_at	contig_76140_1	ANAC022, NAC1	5.8	9	9	112	16	74	12	16	14	13	13	32	84	45	188
	Mtr.19019.1.S1_at	Medtr4g081870	ANAC029, ATNAP, NAP/senNAC	6.4	124	114	10	11	11	98	14	15	12	12	10	11	11	12
	Mtr.11021.1.S1_at	Medtr5g041940.1	ANAC029, ATNAP, NAP/senNAC	6.5	102	43	14	9	8	321	40	123	199	437	502	472	306	914

(b)

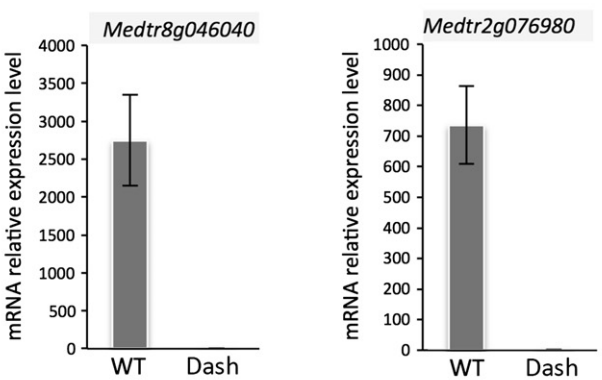

(c)

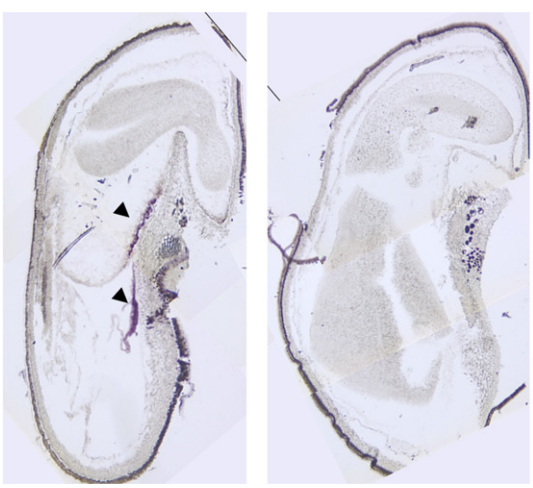

Figure 4. A cysteine-rich peptide (CRP) gene expressed in the chalazal endosperm is strongly repressed in the *dash* mutant seeds.
(a) List of the most down-regulated and up-regulated genes in 8 DAP *dash* pods compared with WT. Tissue expression data from the *Medicago truncatula* Gene Expression Atlas were added.
(b) Down-regulation of the Mtr.21576.1.S1_at and Mtr.1254.1.S1_at probes set (CRP genes *Medtr8g046040* and Medtr2g076980 respectively) in *dash* seeds compared with WT by qRT-PCR. *ACTIN PDF2* and *GAPDH* were used as reference genes for expression levels normalization.
(c) *In situ* hybridization of the CRP gene *Medtr8g046040* in the chalazal endosperm (arrowheads) of WT 12 DAP seeds. Hybridization with the control sense probe (right) did not yield to any signal.

catabolism (Figure 5b) (Ludwig-Müller, 2011). Similar observations were made for the NF5285 mutant pods, which possessed 11-fold higher auxin content than WT pods (Figure S8).

In view of the abnormal accumulation of auxin in mutant pods during embryogenesis, we tested the effects of exogenous IAA and TIBA (2,3,5-triiodobenzoic acid) treatments to assess the integrity of IAA polar transport/signaling in mutant lines. Exogenous treatments with IAA on 6 DAP mutant pod led to rescue of the lethal phenotype but only partially complemented the seed/pod size phenotype (Figure 5c,d). These treatments mimicked the partial restoration of WT phenotype observed at the end of plant life of EMS109. No significant changes were observed when applying these treatments to WT plants. When applying TIBA, an inhibitor of auxin efflux transport, however, we observed a significant decrease of mature pod and seed weights, suggesting that auxin is required for normal seed development and disturbed auxin transport could be a partial explanation of impaired EMS109 seed development. TIBA treatments of WT pods mimicked the *dash* phenotype while exogenous IAA restored pod and seed set, consistent with our transcriptomic results that in the mutant pods auxin efflux transport (i.e. the PIN transporters) was impaired.

DISCUSSION

DASH, an integrator between endosperm and embryo development

The *M. truncatula* gene *DASH*, which encodes a TF from the DOF family, is specifically expressed in the endosperm during embryogenesis (Figure 1). Mutations within the *DASH* sequence resulted in altered embryo growth

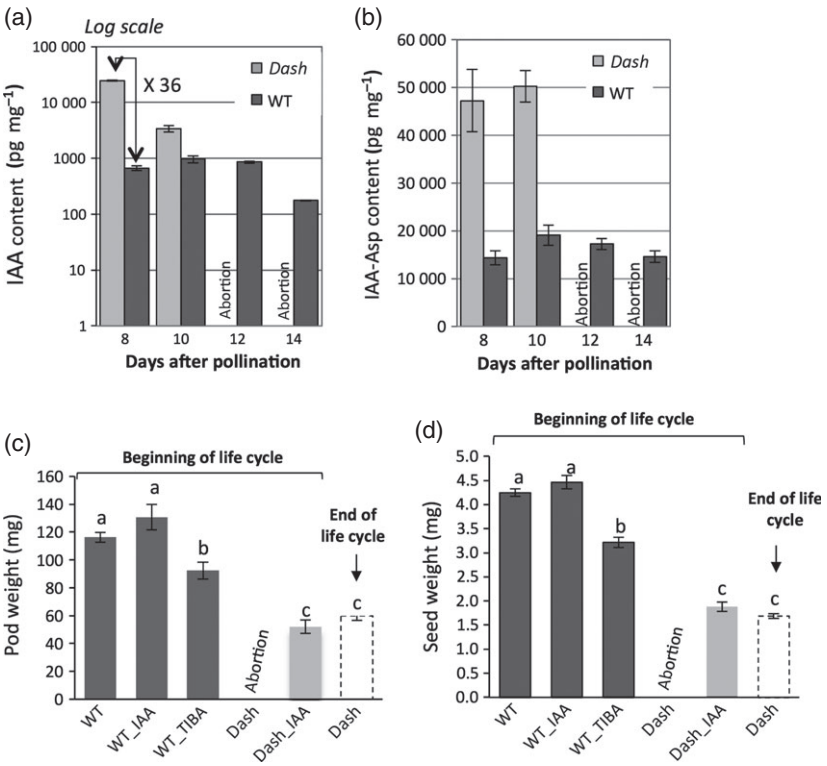

Figure 5. Hormone dosage and treatment effect on pods of EMS109 versus WT.
IAA (a) and IAA-Asp (b) dosages in pods of EMS109 and WT. Effect of exogenous IAA and TIBA treatments on pod (c) and seed (d) weights of EMS109 and WT.

(Figure 3), either resulting in growth arrest at the globular stage and premature pod abscission (NF6042 and EMS109) or smaller seed size (NF5285). This result is reminiscent of previous data reporting that endosperm cellularization and embryo development are closely related, and probably link *via* nutrient translocation to determine final seed size (Hehenberger *et al.*, 2012). Contrary to the *mini3* mutant of Arabidopsis, which shows precocious endosperm cellularization probably responsible for a reduced seed size (Luo *et al.*, 2005), cellularized endosperm is present in the *dash* mutant at 6 DAP and 8 DAP (Figure 3e,f) but gradually degenerates, leading to tissue collapse, desiccation and finally to abortion (Figures 3g,h and S6). EMS109 mutant plants progressively acquire the ability to develop pods and set seeds, albeit small ones, suggesting a partial physiological reversion of the mutant phenotype at the end of plant life (Figure 2d). We hypothesize here that a physiological switch occurs to reverse the phenotype at the end of plant cycle, and probably linked to a change in regulation of auxin transport or perception. Interestingly, dramatic switches in biosynthesis, metabolism, signaling and response genes controlling hormone homeostasis have already been demonstrated between leaf development and early leaf senescence (van der Graaff *et al.*, 2006).

The exclusive localization of the *DASH* mRNA in the chalazal zone endosperm (CZE) is of particular interest (Figure 1b). In Arabidopsis, this endosperm region is highly enriched for mRNAs specifically expressed during early seed development (Belmonte *et al.*, 2013). The authors identified transcripts for ubiquitin-dependent protein catabolism genes and enzymes for the biosynthesis of gibberellic acid, abscisic acid, and cytokinin, consistent with other reports showing that hormone metabolism genes are expressed in the CZE (Miyawaki *et al.*, 2004; Hu *et al.*, 2012; Li *et al.*, 2013). Because of the importance of these hormones for seed development, it was proposed that the CZE may serve as a communication hub that integrates developmental processes within the seed (Belmonte *et al.*, 2013). The loss of expression of CZE-specific genes in *dash* suggests that this endosperm sub-region is severely affected in the mutant, and is consistent with associated developmental effects of the embryo.

DASH, a central regulator of early seed developmental processes

A comparison of the transcriptome of developing pods from WT and EMS109 mutant revealed major changes in expression of genes involved in hormone metabolism, protein synthesis and degradation, cell cycle and DNA/chromatin remodelling (Table 2). Many genes expressed early during seed development and involved in cell division were down-regulated in *dash* (Table 2), including cyclin-dependent protein kinase regulators (genes orthologous of CYCD, CYCB, CYCA,), and cytoskeletal proteins (kinesin and phragmoplast-associated kinesin, tubulin, fimbrin). Cyclin and CDK genes have been shown to be over-represented in proliferating endosperm tissue (Day *et al.*, 2008), as syncytial development requires a rapid progression

through the cell cycle, suppression of phragmoplast formation and uncoupling of cytokinesis and mitosis. In addition alteration of cell division in the *dash* mutant was confirmed by the lower number of cells observed in cotyledons of mature seeds (Figure 2f). Genes involved in DNA synthesis and cell wall deposition were also mainly down-regulated in *dash*, which is consistent with the impairment of formation of normal cellular structures observed in *dash* endosperm (Figure S6). Our transcriptomics data also highlighted a specific class of genes whose expression was greatly reduced in the *dash* mutant (Figure 4). These genes encode small CRPs and interestingly one of them (Medtr8g046040) was found by *in situ* hybridization to be expressed in the chalazal endosperm, in a pattern identical to *DASH* suggesting that this gene might possibly be involved in the same pathway. CRPs have been assigned diverse roles and some members of this family are implicated in processes such as fertilization, female gametophyte or seed development (Marshall *et al.*, 2011). Recently, Costa *et al.* (2014) identified 180 small CRPs expressed in developing seeds of Arabidopsis. They showed a specific family of peptides, called ESF1 (Embryo Surrounding Factor 1), accumulated before fertilization in central cell gametes and thereafter in embryo-surrounding endosperm cells, required for proper early embryonic patterning by promoting suspensor elongation (Costa *et al.*, 2014). In maize, the CRP *MEG1* is specifically expressed in the basal endosperm transfer layer, functionally equivalent to the CZE in dicotyledons. *MEG1* regulates maternal nutrient translocation into the seed and RNAi lines display smaller seeds (Costa *et al.*, 2012). The *Medicago* genome contains 682 *CRP* genes, 52 of which are exclusively expressed in developing seeds (Tesfaye *et al.*, 2013). The possible role of small peptides such as Medtr8g046040, in early endosperm development remains to be studied.

Deregulation of auxin homeostasis in *dash*

A strict regulation of auxin gradients has been shown to be critical for proper embryo development (Friml *et al.*, 2003). The high concentration of IAA measured in *dash* mutant pods (Figure 5a,b), together with the fact that the class of auxin biosynthesis/catabolism genes was not significantly affected in *dash*, whereas the class of auxin-induced genes was down-regulated, suggests that auxin transport/distribution may be impaired in the mutants. Down-regulation of auxin response factors in mutant pods accumulating high auxin levels may seem contradictory but is explained by a well documented negative feedback regulatory pathway, which reduces sensitivity of cells towards auxin (Benjamins and Scheres, 2008). Increase of IAA in the *dash* mutant is accompanied by an increase of IAA-Asp, an inactive form of auxin (Ludwig-Müller, 2011) and is consistent with the down-regulation of IAR33-like gene expression (Medtr2g100560), which has been shown to possess *in vitro* hydrolase activity against IAA-Asp (Campanella *et al.*, 2008) (Figure 5b and Table S2). The content of this auxin conjugate increases in response to elevated IAA contents such as in the *sur2* mutant in Arabidopsis (Barlier *et al.*, 2000) consistent with its possible catabolic role to maintain IAA homeostasis (Woodward and Bartel, 2005). A similarly high concentration of auxin in seed and fruit of tomato was observed when auxin transport is inhibited by *N*-1-naphthylphthalamic acid (NPA) treatment (Pattison and Catala, 2012) at an early stage of development.

The existence of auxin gradients during fruit growth, with the highest levels of auxin in the seeds, is well documented and, after fruit set, precise spatial and temporal synthesis, transport and action of auxin are required for proper fruit development (Sundberg and Ostergaard, 2009). Auxin distribution is controlled by polar auxin transport mediated by PIN and AUX/LAX proteins, which control cellular auxin efflux and influx respectively (Vanneste and Friml, 2009) and thus the establishment of auxin gradients promoting auxin signaling (Lau and Deng, 2010). Inactivation of auxin efflux carriers is known to result in embryo lethality or severe apical defects depending on the ecotype background (Friml *et al.*, 2003), which is consistent with the down-regulation of four *MtPIN* transporters in *dash* mutant (Table S2). Interestingly, among the few auxin-responsive genes up-regulated in *dash* is *IAA18.* A gain-of-function mutation of this gene alters *PIN1* expression in the apical domain of the embryo in Arabidopsis, indicating that IAA18 disrupts auxin transport and ultimately auxin gradients (Ploense *et al.*, 2009). In the *dash* mutant, pod growth and seed set were recovered upon external application of IAA directly on immature pods of the *dash* mutant, and TIBA treatment of WT pods resulted in decreased seed/pod size (Figure 5c,d). These results support the hypothesis of a link between the *dash* mutation and auxin perception and/or transport deficiency: a defect in auxin efflux transport will lead to auxin accumulation in the immature pod, which will severely disturb auxin homeostasis necessary for proper embryo, seed and pod development. Indirect evidence exists for a relationship between seed size determination and IAA. For instance, larger seeds were generated in Arabidopsis by mutation of *AUXIN RESPONSE FACTOR2* (*ARF2*), which mediates gene expression in response to auxin and represses cell division (Schruff *et al.*, 2006). The nature of the relationship between *DASH*, expressed in endosperm and deregulation of embryo growth, putatively through auxin transport, remains to be clarified. Our data show that *dash* mutants are affected in IAA accumulation and perception, IAA but do not exclude that other hormonal balances may also be impaired and might impact embryo cell division and ultimately final seed size.

EXPERIMENTAL PROCEDURES

Plant growth conditions and harvest of developing pods

All plants were grown under greenhouse conditions in 1.5 L pots filled with a mix of attapulgite:clay beads (60:40). Temperature was controlled to be 20°C during the day and above 18°C during the night. Artificial lighting was supplied to reach 16 h light per day. The plants were not inoculated with *Sinorhizobium* sp. bacteria and were automatically supplied with fertilizers (3.5 N/3.1 P/8.6 K).

Screening for *dash* mutant lines

Medicago truncatula EMS109 mutants was identified from an EMS population containing 4600 M2 lines from cultivar Jemalong A17 by TILLING screening according to Le Signor *et al.* (2009). Nested PCR was conducted using the following inner primers labelled with IRD-700 and IRD-800 dyes: MtDOF-F2 5′-CCAACCA ATAGCAGTAGCAACCG-3′ and MtDOF-R2 5′-GCTGCACCTAGAAA ATCCAAAGAT-3′.

The *M. truncatula Tnt1* mutant population containing more than 20 000 lines from cultivar R108 was screened as described in Cheng *et al.* (2014). *Tnt1* insertions were identified by nested PCR using gene-specific forward primer sequences 5′-AGGGTCCCA TTTCTTTGACTAGT-3′ and 5′-TGACTAGTGCCACCTCATTGTG-3′ and reverse primer sequences 5′-TCACTGAGGAGGATTGAACT CTG-3′ and 5′-TACCATTACCACCAGCACCA-3′.

The *DASH* gene was sequenced in the mutant lines to confirm and precisely locate the mutation. The EMS and *Tnt1* mutant lines were back-crossed with the corresponding WT lines.

In situ hybridization

The method for digoxygenin labelling of RNA probes, tissue preparation and *in situ* hybridization was described by Coen *et al.* (1990) with modifications described by Bradley *et al.* (1993). The *DASH* (Medtr2g014060) and CRP (Medtr8g046040) probes (1125 and 521 bp respectively) included the whole coding sequence and about 50 bp of the 3′ and 5′ untranslated regions. *In vitro* transcription templates were amplified from seed cDNA with the forward primer sequence 5′-TGGCACGTCTCTGTTTAGAAAACGC-3′ and the reverse primer sequence

5′-GATTAATTTCTCAGAGCTATGCTTTC-3′ for *DASH* and with the forward primer sequence

5′-GTCTTTGTAAACCTTTCAAAGTAGCC-3′ and the reverse primer sequence

5′-TTGAGATTGTACAAATATCAACCAC-3′ for the *CRP* gene. The reverse or the forward primer of each pair contained a tail with the T3 promoter at its 5′ end for the production of the anti-sense or sense probe respectively.

Cell size and cell number measurements

Mature seeds were used for cell size and cell number measurements. For cell size determination, seeds were imbibed 4 h in water then overnight in 20% sucrose dissolved in Tris-buffered saline solution (TBS, pH 7.5) at 4°C. Sections (20 μm) were made by cryo-dissection at −20°C (Leica; www.leica-microsystems.com). Sections were stained using toluidine blue and cell density was calculated according to the number of cells per unit area between WT and mutant lines. For cell number determination, imbibed mature seeds were digested for 36 h at 37°C in a enzymatic solution containing 0.45 M sorbitol, 10 mM $MgCl_2$, 1 mM KH_2PO_4, 20 mM MES (pH 5.6), 0.4% Macerozyme R10 (Phytotechnology; www.phytotechlab.com), 1% cellulose Onozuka R10 (Phytotechnology). Cell number of a subset of cell suspension was counted using a haemocytometer and normalized according to the area of the haemocytometer and to the volume of the digestion solution.

Seed clearing

Seeds from plants EMS109, NF6042, NF5285, A17 and R108 were fixed in ethanol/acetic acid (9:1) for 1 h, transferred to 90% ethanol for 1 h then 70% ethanol for 1 h. Treated seeds were transferred onto microscope slides and covered with a chloral hydrate solution (4 g chloral hydrate, 0.5 ml glycerol 100%, 1 ml water) for 4 h and observed with a Zeiss Axiophot photomicroscope equipped with Nomarski DIC optics.

Light microscopy

Developing seeds (8–10 DAP) from *dash* and WT plants were vacuum-infiltrated overnight at 4°C with a fixative mixture containing 3% (v/v) gluteraldehyde and 2% (w/v) paraformaldehyde in 0.1 M sodium phosphate-buffered medium (pH 7.2). Seeds were then washed and dehydrated in an ethanol series before embedding in Historesin following provider's instructions. Thick sections (1 μm) were stained with 0.1% (w/v) toluidine blue plus 0.5% (w/v) methylene blue prior to examination by bright field microscopy with a microscope (Leica).

Complementation of *dash* mutant plants

A fragment of 1150 bp of the native promoter with the 1011 bp of the coding sequence of *MtDASH* was amplified by PCR using primers F-TGTAATACTAATGTTTTCTTGACTG and R-CTGAGGAG GATTGAACTCTGACAG. The *pDASH::DASH* construct was introduced into the pMDC123 vector (Curtis and Grossniklaus, 2003). The leaves of *M. truncatula* (A17) mutants were infected with *A. tumefaciens* EHA105 strain harbouring the complementation vector (Cosson *et al.*, 2006). Resistant calluses obtained after 1–1.5 month of selection were transferred onto regeneration medium. The regenerated shoots or plantlets obtained after 3–4 months were transferred to half-strength SH9 medium supplemented with 1 mg/L IAA. All the regenerating cultures were kept at 25°C under fluorescent light (140 $\mu E\ m^{-2}\ s^{-1}$) at a photoperiod of 16 h in the growth chamber. After 3–4 weeks, plants were transferred to soil and grown in the greenhouse (16 h light, 390 $\mu E\ m^{-2}\ s^{-1}$).

Affymetrix microarray, data extraction, and normalization

Total RNA was extracted using a modified cetyltrimethylammonium bromide method (Verdier *et al.*, 2008). Next, 5 μg of total RNA from each sample was purified (RNeasy MinElute Cleanup kit; Qiagen; www.qiagen.com) according to the manufacturer's instructions. The Affymetrix *M. truncatula* GeneChip Array (Affymetrix; www.affymetrix.com) was used for expression analysis during seed development. RNA from three independent biological replicates were analysed for each time point. Probe synthesis/labelling, array hybridization, scanning, and data normalization were performed as described by Benedito *et al.* (2008). Raw and normalized microarray data were deposited at Gene Expression Omnibus (GEO, http://www.ncbi.nlm.nih.gov/geo/) as GSE58117. To identify probe sets differentially expressed in *dash* mutant versus WT control, the R package ANAPUCE (J. Aubert, UMR 518 AgroParisTech/INRA) was used. *P*-values were adjusted by the Benjamini–Hochberg method (Benjamini and Hochberg, 1995). Transcripts were considered as differentially expressed when associated with a *P*-value ≤0.05. Over-representation analysis were performed using PAGEMAN software (Usadel *et al.*, 2006). Data were subjected to a

bin-wise Wilcoxon test and resulting *P*-values adjusted according to Benjamini–Hochberg criteria.

cDNA synthesis and quantitative real-time PCR analysis

Two μg of total RNA were treated with RNase-free DNase RQ1 (Promega; www.promega.com) according to the manufacturer's instructions. First-strand cDNA was produced using iScript reverse transcriptase (Bio-Rad; www.bio-rad.com) according to the manufacturer's instructions. qRT-PCR was performed on LightCycler 480 (Roche; www.usdiagnostics.roche.com) using Go*Taq* qPCR Master Mix (Promega, Madison, USA). Next, 1 μl cDNA and 200 nM of each gene-specific primer in a final volume of 5 μl, were incubated at: 95°C for 5 min; and 40 cycles of 95°C for 10 sec and 60°C for 1 min. Relative expressions were normalized against *ACTIN*, *GAPDH*, *MSC27* and *PDF2* expressions using the $2^{-\Delta\Delta C_T}$ method (Livak and Schmittgen, 2001). Each expression profile was repeated three times (three biological replicates) in three technical repetitions.

Phytohormone content measurements and auxin treatments

Pods were ground using a pestle and mortar and 50 mg of tissue powder were used for phytohormone quantification. Phytohormones were extracted using 1 ml of extraction solvent (isopropanol:water:HCl at the ratio 2:1:0.002). Internal standard (50 pg) of d5-IAA was added to the extraction buffer. Extractions were performed by shaking samples at 4°C for 1 h, then 0.5 ml of dichloromethane was added and samples were shaken for another 30 min. After centrifugation at 2900 ***g*** (30 min at 4°C), bottom layers were collected and dried under nitrogen. Dry pellets were resuspended in 0.1 ml methanol and 1 ml of acetic acid 1% then cleaned using conditioned Waters Oasis HLB columns according to manufacturer's instructions (Waters; www.waters.com). Hormone samples were eluted from the columns using 1.8 ml of 80% methanol containing 1% acetic acid to glass vials, dried under nitrogen. Dry samples were dissolved in 25 μl methanol and 25 μl 1% acetic acid and 10 μl was injected in an Agilent triple quadrupole LC/MSMS analyser. A reverse phase 1.7 μm UPLC BEH C18 (2.1 × 150 mm) column was used for separation. Data were analysed using MASSHUNTER quantitative analysis software (Agilent; www.agilent.com).

Individual flowers (50–100) were tagged and developing pods were treated at 6 DAP by immersion in water, IAA (570 μM) or TIBA (200 μM) solution supplemented with a drop of Tween-20. Pods were harvested at maturity and weight measurement was performed on about 20 pods containing seeds.

Distance analysis

The tree was created using full-length DOF coding sequences of proteins from *A. thaliana*, *Glycine max*, *M. truncatula*, *P sativum* and cereals. These protein sequences were aligned and organized based on sequence similarities of the full-length DOF protein sequences by the CLUSTALW algorithm using CLC Genomics workbench software (CLC bio-CLC sequence viewer 6.2, Aarhus, Denmark; www.clcbio.com). Protein sequences are provided in Table S3.

ACKNOWLEDGEMENTS

We would like to thank Peter Rogowsky and Bertrand Dubreucq for helpful advice, Lloyd Sumner and David Huhman for their help in measuring phytohormone content, and Yuhong Tang and Stacy Allen for their assistance with microarray hybridizations. This project has received funding from the European Union (FP7 grant agreement n° 613551) and the Samuel Roberts Noble Foundation. MN was funded by an INRA BAP - Burgundy Region Ph.D studentship.

SUPPORTING INFORMATION

Additional Supporting Information may be found in the online version of this article.

Figure S1. Expression of *DASH* in different plant organs and in seed tissues.

Figure S2. Distance analysis of DOF proteins.

Figure S3. Position of the EMS mutation and of the *Tnt1* insertions within the *DASH* sequence.

Figure S4. Genetic and molecular analysis of the *dash* mutants.

Figure S5. Complementation of EMS109 mutant.

Figure S6. Microscopic observations of embryo and endosperm at 8 DAP from WT (a, c) and EMS109 (b, d) seeds.

Figure S7. Delay in embryo growth in NF5285 mutant seeds.

Figure S8. IAA dosage on pods of NF5285 versus WT from 8 to 12 DAP.

Table S1. List of differentially expressed genes at 8 DAP in *dash* pods compared to WT.

Table S2. List of differentially expressed genes belonging to the "auxin" functional class.

Table S3. List of the 96 DOF protein sequences used to compute the distance analysis in Figure S2.

REFERENCES

Adamski, N.M., Anastasiou, E., Eriksson, S., O'Neill, C.M. and Lenhard, M. (2009) Local maternal control of seed size by KLUH/CYP78A5-dependent growth signaling. *Proc. Natl Acad. Sci. USA*, **106**, 20115–20120.

Assaad, F.F., Mayer, U., Wanner, G. and Jürgens, G. (1996) The KEULE gene is involved in cytokinesis in Arabidopsis. *Mol. Gen. Genet.* **253**, 267–277.

Barlier, I., Kowalczyk, M., Marchant, A., Ljung, K., Bhalerao, R., Bennett, M., Sandberg, G. and Bellini, C. (2000) The SUR2 gene of *Arabidopsis thaliana* encodes the cytochrome P450 CYP83B1, a modulator of auxin homeostasis. *Proc. Natl Acad. Sci. USA*, **97**, 14819–14824.

Belmonte, M.F., Kirkbride, R.C., Stone, S.L. *et al.* (2013) Comprehensive developmental profiles of gene activity in regions and subregions of the Arabidopsis seed. *Proc. Natl Acad. Sci. USA*, **110**, E435–E444.

Benedito, V.A., Torres-Jerez, I., Murray, J.D. *et al.* (2008) A gene expression atlas of the model legume *Medicago truncatula*. *Plant J.* **55**, 504–513.

Benjamini, Y. and Hochberg, Y. (1995) Controlling the false discovery rate – a practical and powerful approach to multiple testing. *J. R. Stat. Soc. Series B Stat. Methodol.* **57**, 289–300.

Benjamins, R. and Scheres, B. (2008) Auxin: the looping star in plant development. *Annu. Rev. Plant Biol.* **59**, 443–465.

Bradley, D., Carpenter, R., Sommer, H., Hartley, N. and Coen, E. (1993) Complementary floral homeotic phenotypes result from opposite orientations of a transposon at the plena locus of *Antirrhinum*. *Cell*, **72**, 85–95.

Campanella, J., Smith, S., Leibu, D., Wexler, S. and Ludwig-Müller, J. (2008) The auxin conjugate hydrolase family of *Medicago truncatula* and their expression during the interaction with two symbionts. *J. Plant Growth Regul.* **27**, 26–38.

Cheng, Y., Dai, X. and Zhao, Y. (2007) Auxin synthesized by the YUCCA flavin monooxygenases is essential for embryogenesis and leaf formation in Arabidopsis. *Plant Cell*, **19**, 2430–2439.

Cheng, X., Wang, M., Lee, H., Tadege, M., Ratet, P., Udvardi, M., Mysore, K.S. and Wen, J. (2014) An efficient reverse genetics platform in the model legume *Medicago truncatula*. *New Phytol.* **201**, 1065–1076.

Coen, E.S., Romero, J.M., Doyle, S., Elliott, R., Murphy, G. and Carpenter, R. (1990) *floricaula*: A homeotic gene required for flower development in antirrhinum majus. *Cell*, **63**, 1311–1322.

Cosson, V., Durand, P., d'Erfurth, I., Kondorosi, A. and Ratet, P. (2006) Medicago truncatula transformation using leaf explants. *Methods Mol. Biol. (Clifton, N.J.)*, **343**, 115–127.

Costa, L.M., Yuan, J., Rouster, J., Paul, W., Dickinson, H. and Gutierrez-Marcos, J.F. (2012) Maternal control of nutrient allocation in plant seeds by genomic imprinting. *Curr. Biol.* **22**, 160–165.

Costa, L.M., Marshall, E., Tesfaye, M. *et al.* (2014) Central cell-derived peptides regulate early embryo patterning in flowering plants. *Science*, **344**, 168–172.

Curtis, M.D. and Grossniklaus, U. (2003) A gateway cloning vector set for high-throughput functional analysis of genes in planta. *Plant Physiol.* **133**, 462–469.

Day, R.C., Herridge, R.P., Ambrose, B.A. and Macknight, R.C. (2008) Transcriptome analysis of proliferating Arabidopsis endosperm reveals biological implications for the control of syncytial division, cytokinin signaling, and gene expression regulation. *Plant Physiol.* **148**, 1964–1984.

D'Erfurth, I., Le Signor, C., Aubert, G. *et al.* (2012) A role for an endosperm-localized subtilase in the control of seed size in legumes. *The New Phytol.* **196**, 738–751.

Diaz, I., Vicente-Carbajosa, J., Abraham, Z., Martínez, M., Isabel-La Moneda, I. and Carbonero, P. (2002) The GAMYB protein from barley interacts with the DOF transcription factor BPBF and activates endosperm-specific genes during seed development. *Plant J.* **29**, 453–464.

Fiume, E. and Fletcher, J.C. (2012) Regulation of Arabidopsis embryo and endosperm development by the polypeptide signaling molecule CLE8. *Plant Cell*, **24**, 1000–1012.

Forestan, C. and Varotto, S. (2011) The role of PIN auxin efflux carriers in polar auxin transport and accumulation and their effect on shaping maize development. *Mol. Plant*, **5**, 787–798.

Forestan, C., Meda, S. and Varotto, S. (2010) ZmPIN1-mediated auxin transport is related to cellular differentiation during maize embryogenesis and endosperm development. *Plant Physiol.* **152**, 1373–1390.

Friml, J., Vieten, A., Sauer, M., Weijers, D., Schwarz, H., Hamann, T., Offringa, R. and Jurgens, G. (2003) Efflux-dependent auxin gradients establish the apical-basal axis of Arabidopsis. *Nature*, **426**, 147–153.

Gallardo, K., Firnhaber, C., Zuber, H., Hericher, D., Belghazi, M., Henry, C., Kuster, H. and Thompson, R. (2007) A combined proteome and transcriptome analysis of developing *Medicago truncatula* seeds: evidence for metabolic specialization of maternal and filial tissues. *Mol. Cell Proteomics*, **6**, 2165–2179.

Garcia, D., Fitz Gerald, J.N. and Berger, F. (2005) Maternal control of integument cell elongation and zygotic control of endosperm growth are coordinated to determine seed size in Arabidopsis. *Plant Cell*, **17**, 52–60.

Geisler-Lee, J. and Gallie, D.R. (2005) Aleurone cell identity is suppressed following connation in maize kernels. *Plant Physiol.* **139**, 204–212.

Hehenberger, E., Kradolfer, D. and Köhler, C. (2012) Endosperm cellularization defines an important developmental transition for embryo development. *Development*, **139**, 2031–2039.

Hu, Y.F., Li, Y.P., Zhang, J.J., Liu, H.M., Tian, M.L. and Huang, Y.B. (2012) Binding of ABI4 to a CACCG motif mediates the ABA-induced expression of the *ZmSSI* gene in maize (*Zea mays* L.) endosperm. *J. Exp. Bot.* **63**, 5979–5989.

Ingram, G.C. (2010) Family life at close quarters: communication and constraint in angiosperm seed development. *Protoplasma*, **247**, 195–214.

Lau, O.S. and Deng, X.W. (2010) Plant hormone signaling lightens up: integrators of light and hormones. *Curr. Opin. Plant. Biol.* **13**, 571–577.

Lauber, M.H., Waizenegger, I., Steinmann, T., Schwarz, H., Mayer, U., Hwang, I., Lukowitz, W. and Jürgens, G. (1997) The Arabidopsis KNOLLE protein is a cytokinesis-specific syntaxin. *J. Cell Biol.* **139**, 1485–1493.

Le Signor, C., Savois, V., Aubert, G. *et al.* (2009) Optimizing TILLING populations for reverse genetics in *Medicago truncatula*. *Plant Biotechnol. J.* **7**, 430–441.

Li, J., Nie, X., Tan, J.L.H. and Berger, F. (2013) Integration of epigenetic and genetic controls of seed size by cytokinin in Arabidopsis. *Proc. Natl Acad. Sci. USA*, **110**, 15479–15484.

Livak, K.J. and Schmittgen, T.D. (2001) Analysis of relative gene expression data using real-time quantitative PCR and the $2^{-\Delta\Delta C_T}$ method. *Methods*, **25**, 402–408.

Ludwig-Müller, J. (2011) Auxin conjugates: their role for plant development and in the evolution of land plants. *J. Exp. Bot.* **62**, 1757–1773.

Luo, M., Dennis, E.S., Berger, F., Peacock, W.J. and Chaudhury, A. (2005) (IKU2), a leucine-rich repeat (LRR) KINASE gene, are regulators of seed size in Arabidopsis. *Proc. Natl Acad. Sci. USA*, **102**, 17531–17536.

Marshall, E., Costa, L.M. and Gutierrez-Marcos, J. (2011) Cysteine-rich peptides (CRPs) mediate diverse aspects of cell-cell communication in plant reproduction and development. *J. Exp. Bot.* **62**, 1677–1686.

Miyawaki, K., Matsumoto-Kitano, M. and Kakimoto, T. (2004) Expression of cytokinin biosynthetic isopentenyltransferase genes in Arabidopsis: tissue specificity and regulation by auxin, cytokinin, and nitrate. *Plant J.* **37**, 128–138.

Möller, B. and Weijers, D. (2009) Auxin control of embryo patterning. *Cold Spring Harb. Perspect. Biol.* **1**, a001545.

Moreno-Risueno, M.A., Martinez, M., Vicente-Carbajosa, J. and Carbonero, P. (2007) The family of DOF transcription factors: from green unicellular algae to vascular plants. *Mol. Genet. Genomics*, **277**, 379–390.

Noguero, M., Atif, R.M., Ochatt, S. and Thompson, R.D. (2013) The role of the DNA-binding One Zinc Finger (DOF) transcription factor family in plants. *Plant Sci.* **209**, 32–45.

Pattison, R.J. and Catala, C. (2012) Evaluating auxin distribution in tomato (*Solanum lycopersicum*) through an analysis of the PIN and AUX/LAX gene families. *Plant J.* **70**, 585–598.

Ploense, S.E., Wu, M.F., Nagpal, P. and Reed, J.W. (2009) A gain-of-function mutation in IAA18 alters Arabidopsis embryonic apical patterning. *Development*, **136**, 1509–1517.

Robert, H.S., Grones, P., Stepanova, A.N., Robles, L.M., Lokerse, A.S., Alonso, J.M., Weijers, D. and Friml, J. (2013) Local auxin sources orient the apical-basal axis in Arabidopsis embryos. *Curr. Biol.* **23**, 2506–2512.

Schruff, M.C., Spielman, M., Tiwari, S., Adams, S., Fenby, N. and Scott, R.J. (2006) The AUXIN RESPONSE FACTOR 2 gene of Arabidopsis links auxin signaling, cell division, and the size of seeds and other organs. *Development*, **133**, 251–261.

Signor, C.L., Savois, V., Aubert, G. *et al.* (2009) Optimizing TILLING populations for reverse genetics in Medicago truncatula. *Plant Biotechnol. J.* **7**, 430–441.

Strompen, G., Kasmi, F.El., Richter, S., Lukowitz, W., Assaad, F.F., Jürgens, G. and Mayer, U. (2002) The Arabidopsis HINKEL gene encodes a kinesin-related protein involved in cytokinesis and is expressed in a cell cycle-dependent manner. *Curr. Biol.* **12**, 153–158.

Sundberg, E. and Ostergaard, L. (2009) Distinct and dynamic auxin activities during reproductive development. *Cold Spring Harb. Perspect. Biol.* **1**, a001628.

Tadege, M., Wen, J.Q., He, J. *et al.* (2008) Large-scale insertional mutagenesis using the Tnt1 retrotransposon in the model legume *Medicago truncatula*. *Plant J.* **54**, 335–347.

Tesfaye, M., Silverstein, K.A., Nallu, S. *et al.* (2013) Spatio-temporal expression patterns of *Arabidopsis thaliana* and *Medicago truncatula* defensin-like genes. *PLoS One*, **8**, e58992.

Thimm, O., Bläsing, O., Gibon, Y., Nagel, A., Meyer, S., Krüger, P., Selbig, J., Müller, L.A., Rhee, S.Y. and Stitt, M. (2004) MapMan: a user-driven tool to display genomics data sets onto diagrams of metabolic pathways and other biological processes. *Plant J.* **37**, 914–939.

Usadel, B., Nagel, A., Steinhauser, D. *et al.* (2006) PageMan: an interactive ontology tool to generate, display, and annotate overview graphs for profiling experiments. *BMC Bioinformatics*, **7**, 535.

van der Graaff, E., Schwacke, R., Schneider, A., Desimone, M., Flügge, U.-I. and Kunze, R. (2006) Transcription analysis of Arabidopsis membrane transporters and hormone pathways during developmental and induced leaf senescence. *Plant Physiol.* **141**, 776–792.

Vanneste, S. and Friml, J. (2009) Auxin: a trigger for change in plant development. *Cell*, **136**, 1005–1016.

Verdier, J., Kakar, K., Gallardo, K., Le Signor, C., Aubert, G., Schlereth, A., Town, C.D., Udvardi, M.K. and Thompson, R.D. (2008) Gene expression profiling of *M. truncatula* transcription factors identifies putative regulators of grain legume seed filling. *Plant Mol. Biol.* **67**, 567–580.

Woodward, A.W. and Bartel, B. (2005) Auxin: regulation, action, and interaction. *Ann. Bot.* **95**, 707–735.

Yanagisawa, S. (2002) The Dof family of plant transcription factors. *Trends Plant Sci.* **7**, 555–560.